Electromagnetic wake fields and beam stability in slab-symmetric dielectric structures

A. Tremaine and J. Rosenzweig
Department of Physics and Astronomy, University of California, Los Angeles, 405 Hilgard Avenue, Los Angeles, California 90095

P. Schoessow
Division of High Energy Physics, Argonne National Laboratory, 9700 South Cass Avenue, Argonne, Illinois 60439

(Received 28 March 1997)

Several promising schemes for high-gradient acceleration of charged particles in slab-symmetric electromagnetic structures have been recently proposed. In this paper we investigate, by both computer simulation and theoretical analysis, the longitudinal and transverse wake fields experienced by a relativistic charged particle beam in a planar structure. We show that in the limit of an infinitely wide beam the net deflecting wake fields vanishes. This result is verified in the limit of a large aspect ratio (sheet) beam by finite beam analysis based on a Fourier decomposition of the current profile, as well as a paraxial wave analysis of the wake fields driven by Gaussian profile beams. The Fourier analysis forms the basis of an examination of flute instability in the sheet beam system. Practical implications of this result for beam stability and enhanced current loading in short-wavelength advanced accelerators are discussed. [S1063-651X(97)01611-5]

PACS number(s): 41.75.Ht, 29.17.+w, 29.27.−a, 41.60.Bq

I. INTRODUCTION

The use of planar structures for advanced accelerator applications has been discussed recently in the context of both metallic, disk-loaded millimeter wave structures for linear collider applications [1] and high gradient dielectric loaded-structures excited by lasers [2]. It has been noted that this type of electromagnetic structure may have advantages over the usual axisymmetry, in ease of external power coupling and lowered space-charge forces [2]. More importantly, it has also been speculated [1,2] that the transverse wake fields associated with this class of structure are mitigated, thus diminishing the beam breakup (BBU) instability which typically limits the beam current in short-wavelength accelerators. This instability arises from off-axis beam current excitation of dipole mode wake fields which in turn steer trailing particles; a measure of the strength of this problem is the amplitude of the transverse wake fields. In this paper we show, by both theoretical and computational analysis, that the transverse wake-field amplitude is in fact diminished for asymmetric ($\sigma_x \gg \lambda_0/2\pi > \sigma_y$, where σ indicates the rms beam size, and $\lambda_0 = 2\pi\omega/c$ is the vacuum wavelength of the electromagnetic wave) relativistic bunched beams. Indeed, in the limit of a structure and beam which is much larger in x than in y, the transverse wake fields vanish, in analogy to the monopole modes of axisymmetric structures.

The organization of this paper is as follows. We begin in Sec. II with some general results which constrain the possible forms of the wake fields, including the relationship of the longitudinal to the transverse wake fields, and the additional implications on the form of the wake fields arising from the vacuum dispersion relation. Wake fields due to beams in the infinitely wide limit are analyzed in Sec. III, with a frequency domain analytical theory compared to computational modeling in the time domain. In Sec. IV, as a first step in the analysis of finite beam effects, we will then provide for a Fourier decomposition of the beam current in x, again employing analytical and computational tools. These results are then compared in Sec. V to those obtained from assumption of a beam current which is Gaussian in x, an analysis which is similar in methodology to that used on paraxial photon beam modes. In Sec. VI, the transverse BBU instability of these beams arising from the dipole modelike wake fields is analyzed in two limits: a single bunch ''flute'' instability, in which ripples in the beam transverse distribution self-amplify, and the multibunch instability due to long-range wakes. We conclude in Sec. VII with a discussion of the practical implications of our results for short-wavelength accelerators, comparing the performance of slab-symmetric and cylindrically symmetric systems from the points of view of beam loading and transverse stability.

II. WAKE FIELDS: GENERAL CONSIDERATIONS

Before we begin an analysis of wake fields which can be excited in slab-symmetric dielectric-loaded structures, we introduce some general considerations concerning the possible forms of these fields. The first of these considerations concerns the relationship between the longitudinal and transverse components of the fields, while the second concerns the constraints on functional form of the field components given by the Maxwell wave equations.

The possible forms of the wake fields left behind a relativistic charged particle, and the net forces imparted by these wake fields on trailing charged particles, are constrained by the Maxwell equations, in ways that were initially described by Panofsky and Wenzel [3]. The original theorem given in Ref. [3] gives a relationship between the integrated longitudinal and transverse momentum kicks a particle receives as it traverses, in the constant-velocity, paraxial limit, an isolated medium or device with an electromagnetic excitation. We generalize this theorem in two ways: (1) we include fields

arising possibly from free charges, assuming that fields and potentials vanish at infinity; and (2) we give an alternate form of the theorem applicable in the infinite medium or structure limit, which is of use when describing a very long interaction between charged particles and their environment. The assumptions leading to these generalized forms of the Panofsky-Wenzel deflection theorem still include, explicitly, that the particle receiving the kick travels parallel to the z axis, with a velocity which is constant.

The net Lorentz force on a charged particle consists of the sum of electric and magnetic components. In general, the electric field $\vec{E}$ may be derived from a scalar potential (ϕ) and a vector potential ($\vec{A}$),

$$\vec{E}=-\frac{1}{c}\frac{\partial\vec{A}}{\partial t}-\vec{\nabla}\phi. \tag{2.1}$$

Inserting Eq. (2.1) into the Lorentz force equation, with the beam particle velocity $\vec{v}_b\equiv\vec{\beta}_b c$ and charge q, we have

$$\vec{F}=q(\vec{F}+\overline{\beta_b}\times\vec{B})\equiv q\vec{W}, \tag{2.2}$$

where, for a particle traveling parallel to the z axis, we may write

$$\beta_b\times\vec{B}=\beta_b\hat{z}\times(\vec{\nabla}\times\vec{A})=\beta_b\left(\vec{\nabla}(A_z)-\frac{\partial\vec{A}}{\partial z}\right). \tag{2.3}$$

We can obtain from Eqs. (2.1)–(2.3) an expression for $\vec{W}$, the net force per unit charge q, as

$$\vec{W}=-\frac{1}{c}\frac{\partial\vec{A}}{\partial t}-\vec{\nabla}\phi+\beta_b\left[\vec{\nabla}(A_z)-\frac{\partial\vec{A}}{\partial z}\right]. \tag{2.4}$$

Using the assumed condition that β_b is constant (an excellent approximation for relativistic beams, $\beta_b\cong 1$) we can express the partial derivatives in Eq. (2.4) in terms of the (convective) full derivative in z,

$$\frac{1}{c}\left(\frac{\partial\vec{A}}{\partial t}+\nu_b\frac{\partial\vec{A}}{\partial z}\right)=\frac{1}{c}\frac{d\vec{A}}{dt}=\beta_b\frac{d\vec{A}}{dz}. \tag{2.5}$$

The full momentum transfer, through a region R, due to the net Lorentz force, can now be rewritten as

$$\Delta\vec{p}=\frac{q}{\beta_b c}\int_R\left[-\beta_b\frac{d\vec{A}}{dz}+\vec{\nabla}(\beta_b A_z-\phi)\right]dz. \tag{2.6}$$

For an isolated system where $\vec{E}$ and $\vec{B}$ are nonvanishing only in the region R, $\vec{A}=0$, when evaluated at the end points of integration. This condition makes the first term inside the integrand in Eq. (2.6) vanish, and we obtain

$$\Delta\vec{p}=\vec{\nabla}\left[\frac{q}{\beta_b c}\int_R(\beta_b A_z-\phi)dz\right]. \tag{2.7}$$

Since the integrated momentum kick field $\Delta\vec{p}$ can be derived from a potential, its curl must vanish,

$$\vec{\nabla}\times(\Delta\vec{p})=0. \tag{2.8}$$

This expression is more usefully written to display the relationship between the longitudinal and transverse kicks,

$$\vec{\nabla}_\perp(\Delta p_z)=\frac{\partial(\Delta\vec{p}_\perp)}{\partial z}. \tag{2.9}$$

It should be noted that this form of the deflection theorem is much more general than that due to Panofsky and Wenzel, in that can be applied to interactions in which free charges and currents come in contact with the beam, such as plasma wake fields [4] and the beam-beam interaction [5]. It states that, for a deflection kick to occur, there must be transverse variation of the longitudinal kick imparted by the fields in the isolated system under consideration.

The equivalent expression of the deflection theorem in the case of continuously applied wave fields can also be derived. Here we make the wave ansatz, that the fields' longitudinal and temporal dependence can be expressed solely in terms of $\zeta=z-\nu_\phi t$. In this case we ignore all transients in the problem, which are in any event covered well by the form of the theorem given in Eq. (2.8). Explicitly examining the curl of the net force on a particle traveling parallel to the z axis with speed ν_b, we have

$$\vec{\nabla}\times\vec{W}=\vec{\nabla}\times(\vec{E}+\vec{\beta}_b\times\vec{B})=\vec{\nabla}\times\vec{E}-(\vec{\beta}_b\cdot\vec{\nabla})\vec{B}=\vec{\nabla}\times\vec{E}+\frac{\beta_b}{\nu_\phi}\frac{\partial\vec{B}}{\partial t}. \tag{2.10}$$

Thus, for $\nu_b=\nu_\phi$, which is always assumed true for wake fields in the relativistic beam limit (a wake field satisfying the wave ansatz must satisfy this condition), we have that the wake field is conservative,

$$\vec{\nabla}\times\vec{W}=\vec{\nabla}\times\vec{E}+\frac{1}{c}\frac{\partial\vec{B}}{\partial t}=\vec{0},\ \text{ or }\ \vec{\nabla}_\perp W_z=\frac{\partial(\vec{W}_\perp)}{\partial\zeta}. \tag{2.11}$$

This form of the theorem basically states that when the wave phase velocity is equal to the beam velocity, a transformation to the rest frame gives a purely electrostatic net force, which is always conservative. Since we are concerned here with a

translationally invariant (in z) structure, we will be more interested in the form of the deflection theorem given by Eq. (2.11). It should also be noted that neither form of the deflection theorem restricts the fields to those arising from the wake of a charged particle beam. In fact, Eq. (2.9) is valid for all localized electromagnetic and electrostatic fields, while Eq. (2.11) applies to any interaction where the beam and wave phase velocity is ultrarelativistic, including wake fields, as well as applied resonant accelerating fields such as those found in most electon linear accelerators.

Equations (2.9) and (2.11) imply that any transverse variation of the longitudinal wake field W_z must produce a transverse wake field $\vec{W}_\perp$ with a nonvanishing longitudinal derivative. Since our analysis below will be concerned with electromagnetic modes separable in Cartesian coordinates, at this point it is useful to recall the dispersion relation governing the variation of the field components,

$$k_x^2+k_y^2+k_z^2=\mu\epsilon\left(\frac{\omega}{c}\right)^2. \tag{2.12}$$

We will examine below the fields acting on charged particles which are (1) located in vacuum, so $\mu=\epsilon=1$; and (2) with ultrarelativistic particle and wake-field phase velocities ($v_b \cong \omega/k_z \cong c$). Under these conditions, Eq. (2.12) yields that $k_x^2=-k_y^2$; if one of the wave numbers is real, the other must be imaginary and of equal amplitude. It should be noted that a more general statement, applicable independent of an assumed symmetry, is that ultrarelativistic wake fields generally obey the two-dimensional Laplace equation $\vec{\nabla}_\perp^2 W_i \cong 0$.

The most interesting limit, from the point of view of the present investigations, in discussing wake fields from ultrarelativistic beams in structures with Cartesian symmetry is the case where W_z has no dependence on one of the transverse coordinates. This corresponds to the physical situation where the structure and beam, and thus electromagnetic wake fields, are infinite and invariant in this coordinate, which we now designate as x. Then we have $k_x=0$, which in turn implies that $k_y=0$, and there is *no* transverse dependence on the longitudinal wake field W_z. Equation (2.11) then implies that the transverse wake field in this case has no longitudinal derivative. Since all components of the wake field are by assumption harmonic in z with a nonvanishing wave number $k_z=\omega/c$, we deduce that the transverse wake field indeed must vanish in this limit. This vanishing of the transverse wake field under the condition of slab symmetry ($\partial/\partial x=0$) can be seen as the analog of the vanishing of the transverse wake-field under the more familiar condition of azimuthal symmetry—$\partial/\partial\theta=0$, for azimuthal mode number $m=0$ (monopole) fields.

This result can also be understood physically in a number of ways, both from the point of view of coupling of the beam to the structure, and the explicit restrictions of the Maxwell equations. In order for the beam to drive transverse wake fields, it must couple to the structure in an asymmetric way when the beam leaves the symmetry ($y=0$) plane. However, the assumption of near speed-of-light beam velocity implies that the beam self-fields collapse to a transversally oriented Lorentz disc. This, combined with an assumed infinitely wide charge distribution, means that a horizontally oriented uniform line charge (the simplest equivalent to a point charge with slab symmetry) has the equivalent field structure of an infinite, uniform sheet of charge. Thus, like the fields arising from an infinite sheet, those arising from an ultrarelativistic line charge are independent of how far away from the line charge the two sides of the structure are; the line charge does not couple asymmetrically to the structure, and no net transverse force is possible.

From the point of view of the Maxwell equations, the following argument also illuminates the physics of the fully slab-symmetric case. With this symmetry, it is clear that there must be no force in the x-direction. This implies that the fields are purely transverse magnetic (TM), because the existence of nonvanishing B_z implies a nonvanishing B_y, as the condition $\vec{\nabla}\cdot\vec{B}=0$ in slab symmetry gives $\partial B_y/\partial y=-\partial B_z/\partial z=-ik_zB_z$. To balance the nonvanishing B_y, and give a vanishing horizontal force, we must have a nonvanishing E_x, which is forbidden by symmetry. Thus we have rigorously shown that, as in the case of azimuthal symmetry, a pure TM field, for which it is straightforward to show also implies that $B_x=-E_y$. For an ultrarelativistic beam, this is the condition for which the net vertical force vanishes. It should be noted that for the isolated systems governed by Eq. (2.9), that the condition imposed on the vertical force is a bit weaker—it must be a constant, not necessarily zero. This, however, clearly represents the case of a static field (the $k_z=0$ limit in the wave case), and thus is not of interest for wake-excited systems.

It should be emphasized again that the strict vanishing of the transverse electromagnetic force is obtained only in the limit of relativistic beam and phase velocities, and for infinitely wide in x slab-symmetric systems. The assumption of relativistic velocities is quite good for nearly all situations of interest; deviations from force cancellation due to finite beam width are studied in detail below.

III. WAKE FIELDS IN THE INFINITE BEAM CASE

The structure considered here, shown in Fig. 1, is a slab-symmetric dielectric-loaded geometry, with a dielectric material of permittivity $\epsilon>1$ ($\mu=1$) in the regions $a\leqslant|y|\leqslant b$, a vacuum gap ($\epsilon=1$), and conducting boundaries at $|y|=b$. This structure is chosen both for ease of calculation and because of the recent interest displayed in this, as well as similar, dielectric-loaded devices [2,6–8]. In the usual fashion, we initially assume that Cerenkov radiation-induced wake fields travel in the beam propagation direction z, with a phase velocity equal to the beam velocity, and with both ultrarelativistic, $v_\phi=v_b\cong c$. Instead of the common Green-function approach to calculation of the wake-field response, however, we will analytically calculate the wake fields by use of energy balance arguments. This approach requires only that we determine the mode characteristics of the structure rather than evaluate rather difficult integrals in the Green-function analysis. The full wake-field response is then found by performing a summation of the wake-field coupling of each mode with a further convolution integral over the beam current profile.

We begin by examining the limiting case of no x dependence of the structure, beam, and resultant electromagnetic

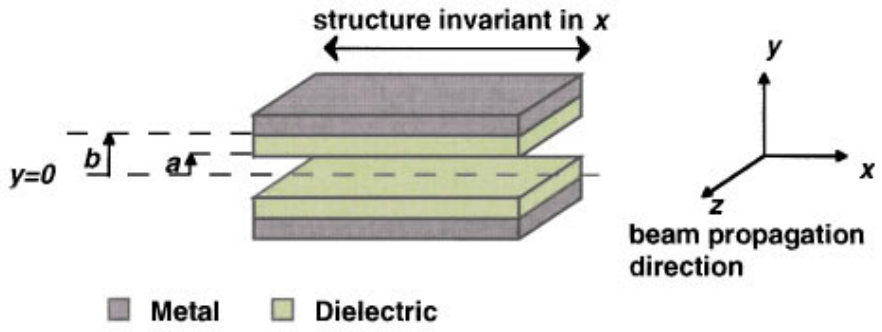

FIG. 1. (Color) Schematic of a slab-symmetric, dielectric-loaded structure, with a vacuum gap half-height a, dielectric layers of permittivity ϵ, and a thickness $b-a$, with metal boundaries at $|y|=b$.

mode, as was done in previous analyses of this two-dimensional problem [9]. By assumption, the longitudinal and temporal dependence of the fields of the nth mode excited by the beam is of the form $\exp[ik_n\zeta]$, where $k_n=\omega_n/c$. As the excited modes in this limit are purely TM, we need only solve for E_z in this analysis. We shall verify in the following sections that this behavior is obtained in the limit of a very wide, yet finite-sized, beam. For the TM case we need only additionally consider the vertical dependence of the longitudinal electric field to determine the mode fields completely. Inside of the gap ($|y|<a$), we have

$$E_{z,n}=E_0\exp[ik_n\zeta], \tag{3.1}$$

with no x or y dependence, where E_0 is an arbitrary amplitude, while in the dielectric ($a<y<b$) we must have

$$E_{z,n}=A_nE_0\exp[ik_n\zeta]\sin[s_{y,n}(y-b)], \tag{3.2}$$

with $s_{y,n}=k_n\sqrt{\epsilon-1}$. Application of the boundary conditions at $y=a$ (continuity of E_z and D_y, which is trivially derived

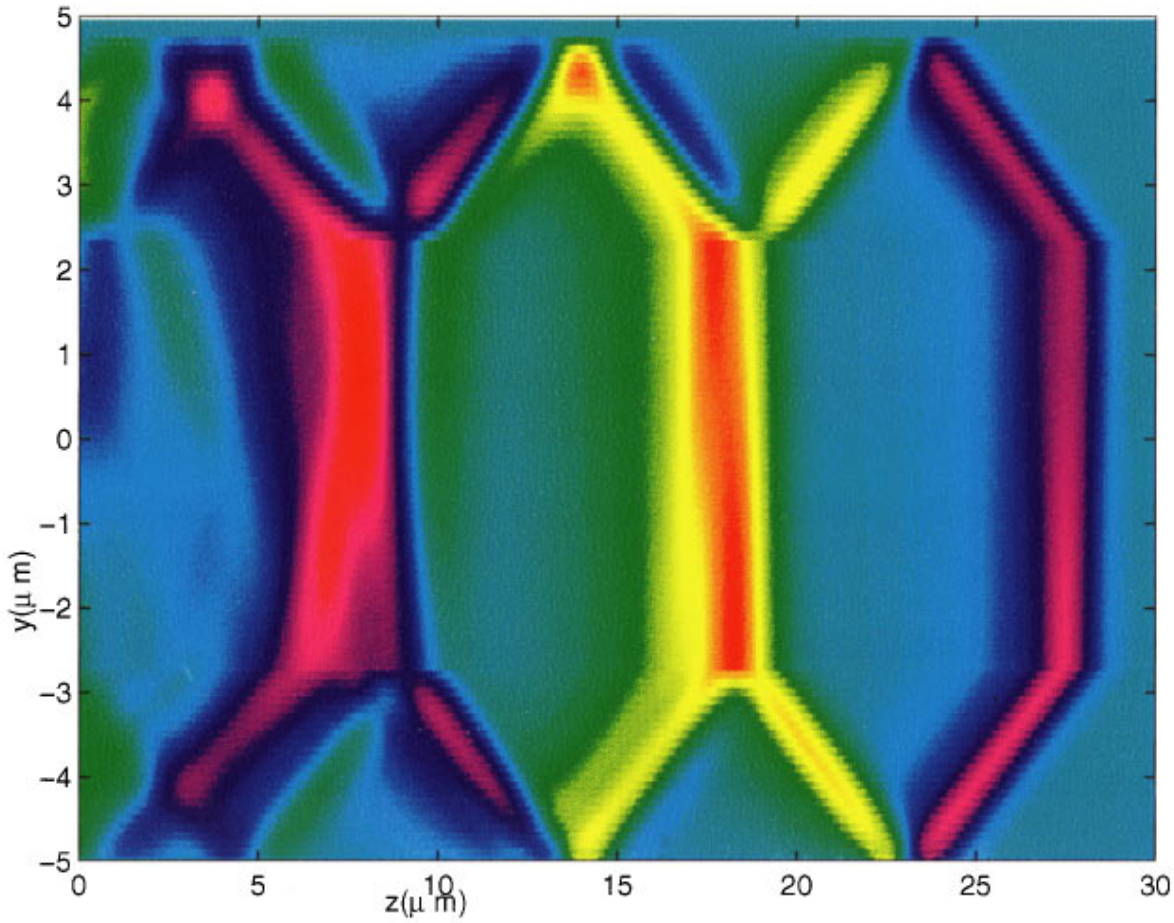

FIG. 2. (Color) False color contour map of W_z for a slab-symmetric structure with a vacuum gap half-height $a=2.5$ μm, a dielectric (of permittivity $\epsilon=4$) in the regions $a<|y|<b$ between the gap and the conducting boundaries at $|y|=b=5$ μm, from time-domain electromagnetic field solver. The ultrarelativistic beam distribution is infinite in x, with a line charge density $\lambda=dq/dx=\sqrt{2/\pi}\sigma_z$, infinitesimal in y (at $y=1$ μm) and Gaussian in z with standard deviation $\sigma_z=0.5$ μm, centered at about $z=27.5$ μm. The color map is linear and in spectral order, with red most negative, violet most positive, and blue-green the zero-field strength.

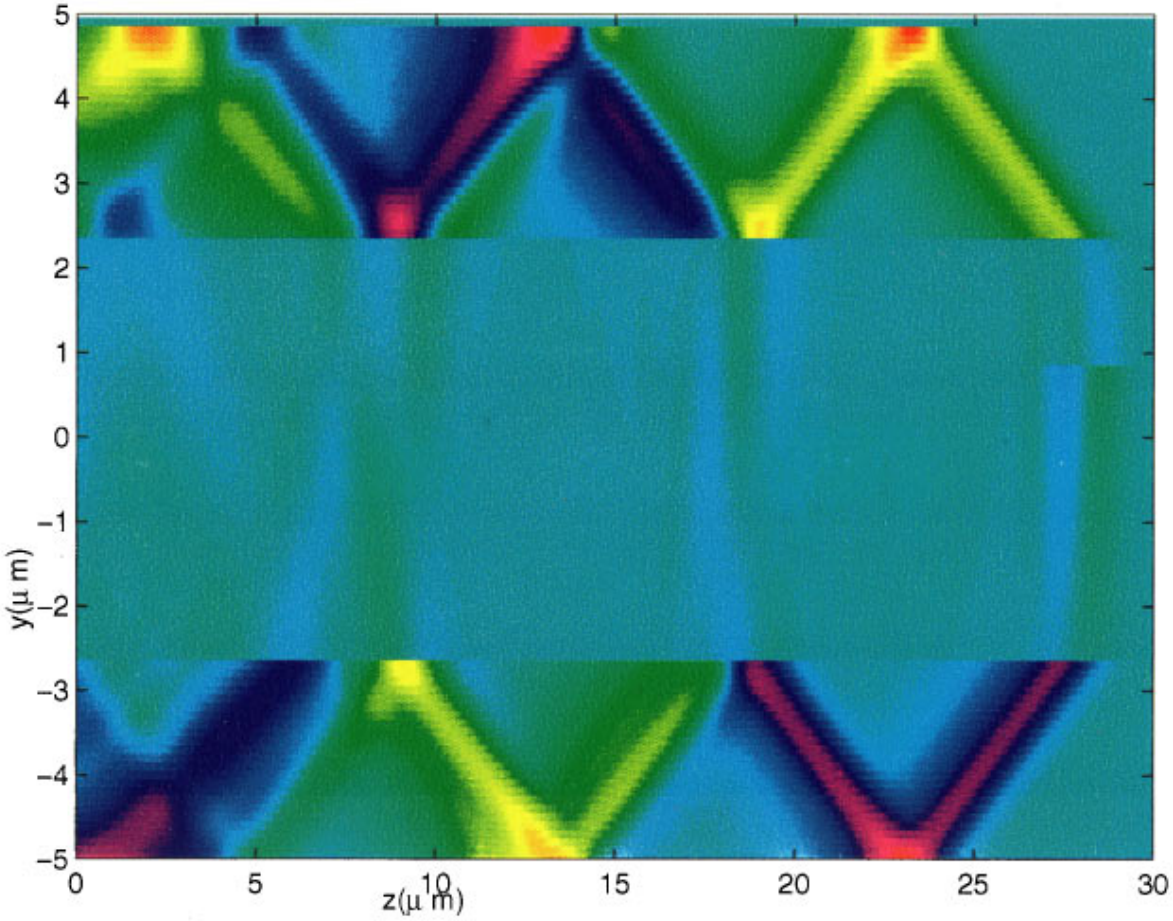

FIG. 3. (Color) False color contour map of W_y for the structure and beam described in Fig. 1. The transverse wake field essentially vanishes in the vacuum gap for an infinitely wide (in x) beam.

from E_z from the relation $\vec{\nabla}\cdot\vec{D}=0$) allows a determination of the eigenvalue of each mode through the transcendental relation

$$\cot[k_n\sqrt{\epsilon-1}(b-a)]=k_n a\,\frac{\sqrt{\epsilon-1}}{\epsilon}, \tag{3.3}$$

and the amplitude of the longitudinal electric field within the dielectric,

$$A_n=\csc[k_n\sqrt{\epsilon-1}(b-a)]. \tag{3.4}$$

Note that, for higher wave-number modes, Eq. (3.3) implies that the phase variation in the dielectric must be approximately $(n+\frac{1}{2})\pi$, and thus A_n becomes large, as the field is concentrated in the dielectric.

Once the fields have been determined, the response of the structure to the passage of an ultrarelativistic, horizontally oriented line charge of constant density $[\rho_e=\lambda\,\delta(y-y_0)\delta(\zeta)]$ within the vacuum gap ($y_0<a$) can be calculated by energy balance. It can be shown that, for a linear wake field [10] the net decelerating field on a line charge associated with a wake amplitude of E_0 is $E_{\rm dec}=E_0/2$. We can equate this energy loss per unit length with the field energy per unit length left behind the ultrarelativistic linear charge density as

$$\lambda E_{\rm dec}=\int(\langle u_{\rm em}\rangle-\langle S_z\rangle)dy, \tag{3.5}$$

where $u_{\rm em}=\frac{1}{2}[\epsilon(E_z^2+E_y^2)+\mu H_x^2]$ is the electromagnetic energy density, $S_z=(4\pi)^{-1}E_yH_x$ is the longitudinal Poynting flux, and $H_x=-\epsilon E_y$. The longitudinal wake field behind the charge obtained from this expression is thus simply

$$W_{z,n}=E_{z,n}=\frac{4\pi\lambda}{a+\epsilon A_n^2(b-a)}\cos[k_n\zeta]\Theta(-\zeta), \tag{3.6}$$

where Θ is the Heaviside function which explicitly shows the causal nature of the wake fields. It should be noted from this expression that the longitudinal wake field is in general largest for the lowest frequency mode. For the slab-symmetric, laser-pumped accelerator proposed in Ref. [2], however, the examples given have the device operating on a higher-frequency mode of the structure. This could pose a beam-loading problem for this and other overmoded laser acceleration schemes, as the beam gains energy from a mode

which it is poorly coupled to, in comparison to the modes which it loses energy to in the form of wake fields.

To obtain the full wake field response from a beam with an arbitrary longitudinal current profile $[\rho_e=\lambda\delta(y-y_0)f(\zeta)]$, we must perform a longitudinal convolution over the point response,

$$W_z=\sum_n \int_\zeta^\infty f(\zeta')W_{z,n}(\zeta'-\zeta)d\zeta'. \tag{3.7}$$

The predictions of Eq. (3.7) have been verified by use of numerical simulation of the wake fields in a planar structure, performed using a custom two-dimensional finite-difference time domain electromagnetic simulation code. The beam is assumed to be a rigid current distribution, infinitesimally thin in the vertical (y) direction and with a fixed offset from the symmetry plane $y=0$. The beam is also taken to be ultrarelativistic and traveling in the $+z$ direction, with a Gaussian longitudinal of standard deviation σ_z. The line charge density of the beam in x is normalized to $\sqrt{2/\pi}\sigma_z$ statcoul/μm, with σ_z in μm. The fields are advanced using the standard leapfrog time integration algorithm. Figure 2 shows a false-color contour map of W_z for a case similar to the infrared wavelength examples given in Ref. [2]. One can clearly see both the uniform speed-of-light phase fronts in the vacuum, and the Cerenkov nature of the wake field in the dielectric, which displays the expected propagation angle. It should also be noted that, even though the beam current is asymmetric with respect to the $y=0$ plane, the excited longitudinal wake is nearly symmetric (after propagation away from the simulation boundary), indicating symmetric coupling of the beam fields to the dielectric and the accompanying suppression of the transverse variations of W_z which lead to a transverse wake field.

Figure 3 shows the net vertical wake field $W_y=E_y+B_x$ excited by the beam in this case; one can see that W_y essentially vanishes inside of the vacuum gap. The lack of full cancellation of E_y+B_x is due mainly to the electric and magnetic field centers in the calculation being one-half of both a spatial and time step apart. Figure 4 displays a comparison between the simulation and analytical results for W_z in this case. The results are in good agreement, with some discrepancies due to the transient fields found in the time-domain simulation which are not present in the Fourier-based analytical treatment.

IV. WAKE FIELDS IN FINITE BEAMS: FOURIER ANALYSIS

With the method of determining the wake-field coupling established in Sec. III, we now turn our attention to wake fields in finite beams. We begin by generalizing the above analysis to a beam of finite horizontal extent by examining the wake fields due to beams of a harmonic (in x) charge profile

$$\rho_{e,k_x}=\lambda(k_x)\cos(k_x x)\,\delta(y-y_0)\,\delta(\zeta), \tag{4.1}$$

where λ is now the peak line charge density. This profile can be viewed as a Fourier component of a finite beam, i.e., $\rho_e(x)=\Sigma\rho_{e,k_x}\cos(k_x x)$, where we implicitly assume that the waveguide now has conducting sidewalls with separation in L_x (allowed wave numbers $k_x=m\pi/L_x$, $m=1,3,5\ldots$), and the beam distribution in x is centered and symmetric within these walls, as is shown in Fig. 5. Partial wake fields obtained from this harmonic analysis can therefore be summed to find the complete wake fields.

The longitudinal electric field associated with the nth mode of the wake fields that the harmonic beam can couple to has the following form in the vacuum region:

$$E_{z,n}=E_0\exp[ik_n\zeta]\times\begin{Bmatrix}\cosh(k_x y)\\ \sinh(k_x y)\end{Bmatrix}\times\cos(k_x x). \tag{4.2}$$

The $\cosh(k_x y)$ dependence indicates the monopolelike, or accelerating, component (independent of y in first order for small vertical offsets) and the $\sinh(k_x y)$ is the dipolelike, or deflecting component, which couples to the longitudinal field with strength approximately linear in y and produces deflecting forces nearly independent of y for small vertical offsets. Note that these modes have explicitly been described as monopolelike and dipolelike—they are exact modes which display a specified multipole characteristic only in lowest order in y.

Since the modes under consideration are not pure TM, but are hybrid modes, we must find the longitudinal magnetic field to specify all the fields. In the gap region, this field has the form

$$B_{z,n}=E_0\exp[ik_n\zeta]\times\begin{Bmatrix}\sinh(k_x y)\\ \cosh(k_x y)\end{Bmatrix}\times\sin(k_x x). \tag{4.3}$$

We again have obviously taken the ultrarelativistic limit, and in this case one must be very careful in finding the transverse components of the fields in the vacuum region. They are

$$E_{x,n}=-i\,\frac{k_n E_0}{2k_x}\exp[ik_n\zeta]\times\begin{Bmatrix}\cosh(k_x y)\\ \sinh(k_x y)\end{Bmatrix}\times\sin(k_x x),$$

$$E_{y,n}=-i\,\frac{k_n E_0}{2k_x}\exp[ik_n\zeta]\times\begin{Bmatrix}\sinh(k_x y)\\ \cosh(k_x y)\end{Bmatrix}\times\cos(k_x x),$$

$$B_{x,n}=iE_0\left(\frac{k_n}{2k_x}-\frac{k_x}{k_n}\right)\exp[ik_n\zeta]\times\begin{Bmatrix}\sinh(k_x y)\\ \cosh(k_x y)\end{Bmatrix}\times\cos(k_x x),$$

$$B_{y,n}=-iE_0\left(\frac{k_n}{2k_x}+\frac{k_x}{k_n}\right)\exp[ik_n\zeta]\times\begin{Bmatrix}\cosh(k_x y)\\ \sinh(k_x y)\end{Bmatrix}\times\sin(k_x x). \tag{4.4}$$

It should be noted that one cannot obtain the case of the uniform beam by taking the limit $k_x\Rightarrow 0$ in Eqs. (4.4), be-

cause these expressions were obtained by assuming that $k_x \gg k_n/\gamma$, where $\gamma=(1-\beta^2)^{-1/2}$ is the Lorentz factor of the beam. One also obtains immediately from Eqs. (4.4) the gratifying result that the transverse forces on a relativistic particle of charge q, due to the modes described by Eqs. (4.2) and (4.3),

$$F_{x,n}\equiv qW_{x,n}=q(E_{x,n}-B_{y,n})=i\,\frac{k_x}{k_n}\,E_0\exp[ik_n\zeta]\times\begin{Bmatrix}\cosh(k_xy)\\ \sinh(k_xy)\end{Bmatrix}\times\sin(k_xx),$$

$$F_{y,n}\equiv qW_{y,n}=q(E_{y,n}+B_{x,n})=-i\,\frac{k_x}{k_n}\,E_0\exp[ik_n\zeta]\times\begin{Bmatrix}\sinh(k_xy)\\ \cosh(k_xy)\end{Bmatrix}\times\cos(k_xx), \tag{4.5}$$

vanish in the limit that $k_x\Rightarrow 0$, as we had found in the uniform line charge ($k_x=0$) beam case. The form of this result could have been directly deduced from the generalized Panofsky-Wenzel theorem given by Eq. (2.11). Equation (4.5) reinforces the primary point of the present analysis. Simply stated, for highly asymmetric (for rms beam sizes $\sigma_x\gg\sigma_y$, with associated $k_x\sim\sigma_x^{-1}$) beams in slab-symmetric structures, transverse wake fields are strongly suppressed. In fact, since all wake fields are proportional to the linear charge density λ, the transverse wake fields scale (at constant charge per bunch) as σ_x^{-2}. This result mitigates one of the major objections to use of high-frequency accelerating structures, that the transverse wake fields scale prohibitively with frequency. This objection holds for cylindrically symmetric structures, but can be greatly eased by use of slab structures.

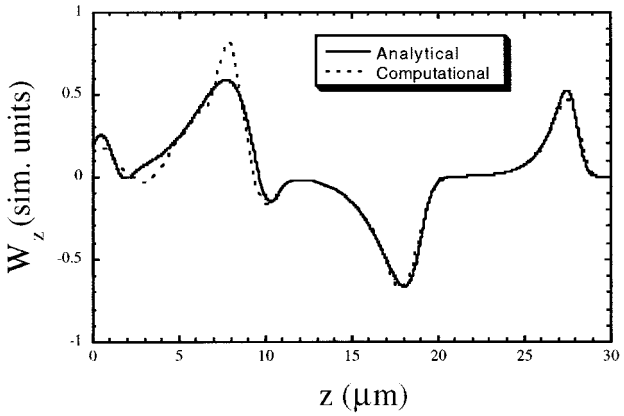

FIG. 4. Comparison of the values of W_z (as a function of z at $y=1$ μm) given by a time-domain electromagnetic field solver and the predictions of Eqs. (3.6) and (3.7), for cases of Figs. 1 and 2.

The fields in the dielectric, unlike those in the gap, can be found by standard wave-guide analysis; for brevity their derivation is omitted. Following the same prescription used to obtain Eqs. (3.1)–(3.3), we obtain a transcendental expression for the eigenvalues of the symmetric modes,

$$\cot[\sqrt{(\epsilon-1)k_n^2-k_x^2}(b-a)]\coth(k_xa)\sqrt{(\epsilon-1)(k_n/k_x)^2-1}-\frac{(\epsilon-1)}{2\epsilon}\left(\frac{k_n}{k_x}\right)^2+1=0. \tag{4.6}$$

The eigenvalues of the antisymmetric modes are simply obtained by substitution of $\tanh(k_xa)$ for $\coth(k_xa)$ in Eq. (2.11). The longitudinal wake fields associated with the symmetric modes are

$$W_{z,n}(k_x)=\frac{4\pi\cosh(k_xy_0)\cosh(k_xy)\cos(k_xx)\cos(k_n\zeta)\Theta(-\zeta)}{\dfrac{\sinh[2k_xa]}{2k_x}\left[\left(\dfrac{k_x}{k_n}\right)^2+1\right]+\left[\dfrac{\epsilon\cosh^2(k_xa)}{\sin^2[s_n(b-a)]}+\dfrac{\sinh^2(k_xa)}{\cos^2[s_n(b-a)]}\right]\left[\left(\dfrac{k_x}{s_n}\right)^2+2\right]\left(\dfrac{b-a}{2}\right)+\cdots}$$
$$\times\cdots\frac{\sin[2s_n(b-a)]}{4s_n}\left[\left[\frac{\sinh^2(k_xa)}{\cos^2[s_n(b-a)]}-\frac{\epsilon\cosh^2(k_xa)}{\sin^2[s_n(b-a)]}\right]\left(\frac{k_x}{s_n}\right)^2+\frac{4\epsilon k_xs_n}{k_n^2(\epsilon-1)}\frac{\cosh(k_xa)\sinh(k_xa)}{\sin[s_n(b-a)]\cos[s_n(b-a)]}\right]; \tag{4.7}$$

those of the antisymmetric modes are obtained by substitution of $\sinh(k_x\tilde{y})$ for $\cosh(k_x\tilde{y})$, and vice versa, where $\tilde{y}$ takes on the values of a, y, and y_0 in Eq. (4.7).

A discrete sum and convolution integral similar to Eq. (3.7) which sums over both symmetric and antisymmetric modes, as well as the beam charge distribution, must be performed to obtain the full wake fields for a beam of finite extent in configuration space. The resultant expressions have also been compared to simulations of this periodic (in x) system, with W_y and W_z obtained by both methods shown in Fig. 6. The algorithm in the numerical simulations used in this case is based on discretizing the Maxwell equations after Fourier transforming with respect to x. The discrepancies in the two approaches due to transient effects are slightly more pronounced in this case, but again the agreement is quite good. Parametric studies performed with these simulations have also verified the suppression of transverse wake fields for wide beams.

The Fourier analysis of the beam current is most appropriate for quantifying the behavior of the wake fields in, e.g.,

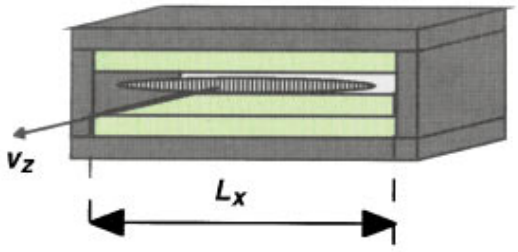

FIG. 5. (Color) Dielectric waveguide with conducting sidewalls of separation in L_x for Fourier beam analysis, with allowed wave numbers $k_x = m\pi/L_x$ ($m = 1,3,5 \ldots$).

millimeter-wave structures [1], which have sidewalls not too distant from the beam. It is also, as will be seen below, most useful for analyzing the flute, or filamentation instability of asymmetric beams in slab-symmetric structures. This work, however, is motivated by the investigation of ultrashort wavelength (infrared to optical) accelerator structures such as those discussed in Ref. [2] in which the sidewalls are very distant from the beam. In order to handle this case, in which the beam current is rather isolated horizontally, we now examine the wake fields generated by a beam with a Gaussian profile. It should be noted that adoption of this physical model has the additional motivation that the Gaussian beam is commonly encountered in practice, as it is produced in systems in thermal equilibrium.

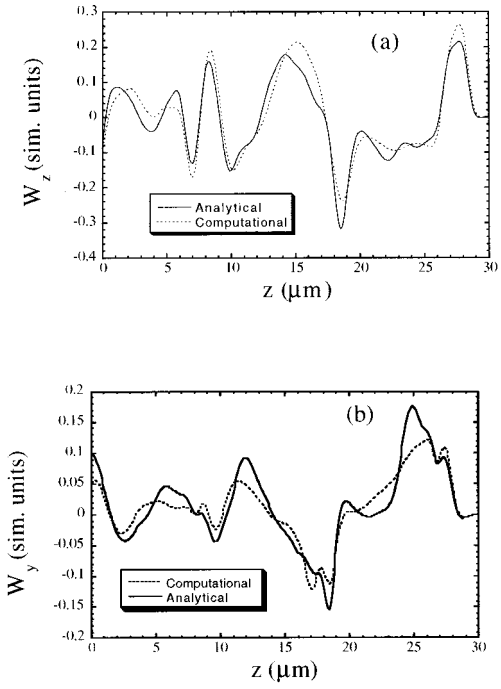

FIG. 6. Comparison of the values of (a) W_z and (b) W_y (as a function of z at $y = 1$ μm) given by the time-domain electromagnetic field solver and the predictions of Eqs. (6) and (12), for the identical structure and beam of Figs. 1–3, but with the beam charge distribution modulated with $k_x = 0.4$ μm^{-1}.

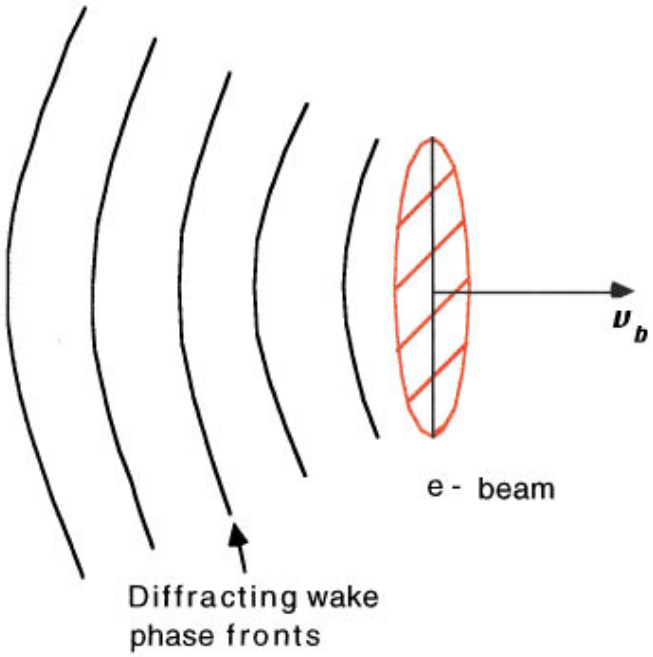

FIG. 7. (Color) Diagram of the wake-field diffraction pattern in the x-z plane, for Gaussian beam and wake-field model calculations.

V. FINITE-BEAM EFFECTS: GAUSSIAN BEAM ANALYSIS

We now turn to the analysis of the wakes produced by the commonly encountered Gaussian horizontal beam profile as it traverses the very wide dielectric structure shown schematically in Fig. 1. The structure is assumed to be wide enough such that the deviation in the wakes due to the finite width effects can be ignored. In this limit, the solutions to the wave equation can be found in the paraxial approximation by utilizing methods developed for analysis of Gaussian photon beams in lasers and optical transport systems.

In the present case, the beam current profile is assumed to have the form

$$\rho_{e,w_{x,n}(\xi)} = \lambda(w_{x,n}) e^{-x^2/w_{x,0}^2} \delta(y - y_0)\, \delta(\zeta), \qquad (5.1)$$

where $w_{x,0} \equiv \sqrt{2}\sigma_{x,b}$ is, following the notation of Siegman [11] for photon beam analysis, the horizontal particle beam size, which is identical to the horizontal width of the wake field extent in x directly behind the exciting line charge ($\zeta = 0-$). This current will drive wake fields which are in many ways similar to Gaussian photon beams, but with some notable differences. In photon beam propagation, the fields are derivable from the paraxial wave equation, and are Gaussian in both transverse coordinates. For the structure induced wake fields, the fields will have a Gaussian dependence in only the x direction, where the paraxial approximation in its familiar form ($k_n w_{x,0} > 1$) can still be employed. Since the solution to the paraxial wave equation is separable in the x and y coordinates with similar types of solutions (Hermite-Gaussian) for each coordinate, one might suppose that the vertical dependence of the fields also be Gaussian. In the limit that $w_x \gg a$, however, the vertical dependence of the

fields is expected to be negligible (of second order in the small parameter $a/w_{x,0}$) and, as in the infinite beam and structure case, the field has no significant vertical dependence in the vacuum gap.

As mentioned above, the horizontal dependence of the longitudinal electric field directly behind the infinitesimally short beam takes the form of the current, $E_z \sim \exp(-x^2/w_{x,0}^2)$. We note that this wake field can be viewed as similar to the wake for the Fourier analysis, Eq. (4.2), in that it has a local maximum in x. In fact, for small $k_x y$, $\cos(k_x x)$, and $\exp(-x^2/w_{x,n}^2)$ are locally equivalent if we substitute $w_{x,n} \Leftrightarrow k_x/2$. Once we have found this local equivalency, in fact, the Gaussian wakes can be found by substitution, exploiting the Fourier wakes as a model. The resulting fields can be verified as being solutions to Maxwell equations in the paraxial limit.

It should also be noted that the above comparison can also be done for the antisymmetric wake field in Eq. (4.2). The dependence of the dipolelike Fourier wake becomes linear in y for small $k_x y$. A linearly dependent wake can be seen to be an acceptable solution to the paraxial wave equation if it is noted that for small y, the first odd-symmetry Hermite-Gaussian solution is also linear. Thus the antisymmetric Gaussian wake can be expressed as $E_z \propto y \exp(-x^2/w_{x,n}^2)$, which is equivalent to the dipole mode described in Eq. (4.2).

The wake fields created by the beam are to be initially at a waist, then diffract out behind the beam, as is shown schematically in Fig. 7. The waist, as well as the entire field pattern, moves forward in z at the speed of the beam $v_z \cong c$. It is again interesting to contrast this form with that of a laser beam. A focused laser beam envelope is minimized at a spatially stationary waist, after which it diffracts away transversely. While the electromagnetic waist of the wake fields is stationary in the beam rest frame, not the laboratory frame, the laser and wake fields hold in common the expected behavior that if one travels with a phase front, diffraction of the fields is observed as time advances.

The full longitudinal (symmetric) wake field in the structure can be found from paraxial wave solutions to be

$$E_{z,n} = E_{0,n} e^{-[x^2/w_{x,n}^2(\zeta)] - ik[x^2/R_n(\zeta)]} \exp[ik_n \zeta + \psi_n(z)] \tag{5.2}$$

where $\psi_n(\zeta) = \tan^{-1}(\zeta/z_{R,n})$ is the Guoy phase shift of a given mode, $z_{R,n} = \pi w_{x,n}^2(0)/\lambda_n = k_n \sigma_x^2$ is its Raleigh (diffraction) length, $R_n(\zeta) = \zeta[1 + (z_{R,n}/\zeta)^2]$ is the local radius of curvature of the phase fronts, and $w_{x,n}^2(\zeta) = w_{x,0}^2[1 + (\zeta/z_{R,n})^2]$ is the horizontal spot size. It should be emphasized that at the point of creation directly behind the beam the diffracting wake field is at a waist. Here the beam size is a minimum, and the Guoy phase shift is most rapidly changing. In light of the dispersion relation Eq. (2.12), this phase shift can be viewed as equivalent to a longitudinal wave-number shift in the region of largest horizontal wave-number k_x.

Using the Fourier wake analysis as a guide, we found the remaining fields in the gap:

$$\begin{aligned}
B_{z,n} &= E_{0,n} \frac{2xy}{w_{x,n}^2(\zeta)} e^{-[x^2/w_{x,n}^2(\zeta)] - ik[x^2/R_n(\zeta)]} \exp[ik_n \zeta + \psi_n(\zeta)], \\
E_{x,n} &= -i \frac{E_{0,n}}{2} (k_n x) e^{-[x^2/w_{x,n}^2(\zeta)] - ik[x^2/R_n(\zeta)]} \exp[ik_n \zeta + \psi_n(z)], \\
E_{y,n} &= -i \frac{E_{0,n}}{2} (k_n y) e^{-[x^2/w_{x,n}^2(\zeta)] - ik[x^2/R_n(\zeta)]} \exp[ik_n \zeta + \psi_n(z)], \\
B_{x,n} &= i \frac{E_{0,n}}{2} \left[1 - \left(\frac{2}{k_n w_{x,n}(\zeta)}\right)^2\right] \\
&\quad \times (k_n y) e^{-[x^2/w_x^2(\zeta)] - ik[x^2/R_n(\zeta)]} \exp[ik_n \zeta + \psi_n(z)], \\
B_{y,n} &= -i \frac{E_{0,n}}{2} \left[1 + \left(\frac{2}{k_n w_{x,n}(\zeta)}\right)^2\right] \\
&\quad \times (k_n x) e^{-[x^2/w_{x,n}^2(\zeta)] - ik[x^2/R_n(\zeta)]} \exp[ik_n \zeta + \psi_n(z)].
\end{aligned} \tag{5.3}$$

The transverse forces associated with these fields,

$$\begin{aligned}
F_{x,n} &\equiv qW_{x,n} = q(E_{x,n} - B_{y,n}) \\
&= iE_0 \frac{2x}{k_n w_{x,n}^2(\zeta)} e^{-x^2/2\sigma_x^2} \exp[ik_n \zeta + \psi(z)], \\
F_{y,n} &\equiv qW_{y,n} = q(E_{y,n} + B_{x,n}) = -iE_0 \frac{2y}{k_n w_{x,n}^2(\zeta)} \\
&\quad \times e^{-y^2/2\sigma_x^2} \exp[ik_n \zeta + \psi(z)],
\end{aligned} \tag{5.4}$$

again will diminish for very wide beams. This result is in good agreement with the analysis of the Fourier beam case, as well as the limiting infinite beam case.

Employing the same techniques as used to derive Eqs. (3.3) and (4.6), we find the transcendental eigenvalue expression for the symmetric Gaussian mode to be

$$\frac{\sigma_x}{a} \cot\left[\left((\epsilon - 1)k_n^2 - \frac{1}{\sigma_x^2}\right)^{1/2} (b - a)\right] \sqrt{(\epsilon - 1)(k_n \sigma_x)^2 - 1} - \frac{(\epsilon - 1)}{2\epsilon} (k_n \sigma_x)^2 + 1 = 0. \tag{5.5}$$

The longitudinal wake-field amplitude is similarly given by

$$W_n=\frac{4\pi\lambda_0}{a\left(1+\frac{1}{2k_n^2\sigma_x^2}\right)+\frac{a^3}{3\sigma_x^2}\left(\frac{1}{k_n^2\sigma_x^2}+\frac{1}{2}\right)+\left[\frac{\varepsilon}{\sin^2[s_n(b-a)]}+\frac{1}{2k_n^2\sigma_x^2(\varepsilon-1)}\left(\frac{\varepsilon}{\sin^2[s_n(b-a)]}-\frac{4s_na}{\sin[2s_n(b-a)]}+\frac{s_n^2a^2}{\cos^2[s_n(b-a)]}\right)\right]\left[\frac{b-a}{2}-\frac{\sin[s_n(b-a)]}{4s_n}\right]+\cdots}$$

$$\times\left[\frac{a^2}{2\sigma_x^2\cos^2[s_n(b-a)]}+\frac{1}{k_n^2(\varepsilon-1)}\left(\frac{\varepsilon s_n^2}{\sin^2[s_n(b-a)]}+\frac{4s_na}{\sigma_x^2\sin[2s_n(b-a)]}+\frac{a^2}{\sigma_x^2\cos^2[s_n(b-a)]}\right)\right]\left[\frac{b-a}{2}+\frac{\sin_n[s(b-a)]}{4s_n}\right], \tag{5.6}$$

and was found using energy balance. The wake fields coming off the beam initially have all energy flowing in the longitudinal direction. As they start to diffract, energy flow is transferred to the transverse directions; thus it was necessary to calculate the wakes when at a waist.

As mentioned above, the Gaussian modes for an antisymmetric profile in y can also be found. The form of the longitudinal electric field is

$$E_z=E_0\frac{\sqrt{2}y}{\omega_{x,n}(\zeta)}e^{-[x^2/w_{x,n}^2(\zeta)]-ik_n[x^2/R_n(\zeta)]}\exp[ik_n\zeta+\psi_n(\zeta)]. \tag{5.7}$$

Following the prescription outlined above, the transverse wakes

$$F_x=ieE_0\frac{2\sqrt{2}xy}{k_n\omega_{x,n}^3(\zeta)}e^{-[x^2/w_{x,n}^2(\zeta)]-ik_n[x^2/R_n(\zeta)]}\exp[ik_n\zeta+\psi_n(\zeta)],$$

$$F_y=-ieE_0\frac{\sqrt{2}}{k_n\omega_{x,n}(\zeta)}e^{-[x^2/w_{x,n}^2(\zeta)]-ik_n[x^2/R_n(\zeta)]}\exp[ik_n\zeta+\psi_n(\zeta)] \tag{5.8}$$

have an associated amplitude of

$$W_n=\frac{4\pi\lambda_0}{a\left(\frac{1}{2}+\frac{1}{k_n^2\sigma_x^2}\right)+\frac{a^3}{3\sigma_x^2}\left(\frac{1}{2k_n^2\sigma_x^2}+1\right)+\left[\frac{\varepsilon a^2}{\sigma_x^2\sin^2[s_n(b-a)]}+\frac{1}{2k_n^2(\varepsilon-1)}\left(\frac{\varepsilon a^2}{\sigma_x^4\sin^2[s_n(b-a)]}-\frac{4s_na}{\sigma_x^2\sin[2s_n(b-a)]}+\frac{s_n^2}{\cos^2[s_n(b-a)]}\right)\right]\left[\frac{b-a}{2}-\frac{\sin[s_n(b-a)]}{4s}\right]+\cdots}$$

$$\times\left[\frac{1}{2\cos^2[s_n(b-a)]}+\frac{1}{k_n^2(\varepsilon-1)}\left(\frac{\varepsilon s_n^2a^2}{\sigma_x^2\sin^2[s_n(b-a)]}+\frac{4s_na}{\sigma_x^2\sin[2s_n(b-a)]}+\frac{1}{\sigma_x^2\cos^2[s_n(b-a)]}\right)\right]\left[\frac{b-a}{2}+\frac{\sin[s_n(b-a)]}{4s_n}\right], \tag{5.9}$$

and we again observe that for wide beams the dipolelike mode transverse wake fields are considerably reduced.

This Gaussian wake analysis can easily be extended to include arbitrary beam profiles by using Hermite-Gaussian functions [11] as a basis set to represent the beam. This allows the analysis of beams which are modulated in x, as in the Fourier case, but with finite extent and no reference to existence of sidewalls. A useful result of this analysis is that a beam with N horizontal modulations has an effective Rayleigh length which is shortened by a factor of $\sqrt{N}$. Thus higher frequency-modulations on a beam create wakes which diffract out more quickly, and the long range wake field is eventually dominated by the lowest spatial frequency (simple Gaussian) component.

VI. TRANSVERSE INSTABILITIES IN ASYMMETRIC BEAMS

With the analysis of the wake-field excitation complete, the wake-field-induced transverse instabilities in very asymmetric beams can now be analyzed. These instabilities fall into two categories: the short-range, single-bunch beam breakup (BBU) instability which tends to ripple or ''flute'' the charge distribution in x with a fairly large wave number ($k_x \sim a^{-1}$), which couple most strongly to the structure but diffract away quickly, and the long-range, multibunch BBU instability, in which the Gaussian wakes of the bunches as a whole, rather than horizontal Fourier structure of the bunches, are dominant. These instabilities are analyzed following the formalisms developed for the flute instability by Whittum [12], using our results on the Fourier components of the wakes, and for the multibunch BBU by Thompson and Ruth [13] using the Gaussian wake analysis of Sec. V.

We begin by examining the flute instability, employing the physical and mathematical model of the beam dynamics developed in Ref. [12] to analyze this type of instability in the dense beam-plasma interaction. In this model, the beam is viewed in lowest order as a uniform slab lying symmetrically about the symmetry plane of the device. A more detailed analysis, in which the beam is not taken to be uniform in x, with a harmonic perturbation, but instead is modeled as a Gaussian with periodic perturbations may be performed by use of Hermite-Gaussian functions. It should be emphasized that we do not mean to imply that we are discussing the physically uninteresting case of a uniform sheet beam with a sharp cutoff horizontal edge, which would have significant Fourier components which would drive BBU instability. This type of beam would not in general be found in, e.g., high-energy linear collider beams derived from damping rings, which are approximately thermally equilibrated in all phase planes, giving Gaussian beam profiles. Keeping the model's applicability in mind, a vertical perturbation $\xi(z,\tau)$ of a small amplitude and harmonic (with wavenumber k_x) dependence in x is assumed, which can be shown [12] to be equivalent to a harmonic charge-density perturbation. The wake fields arising from this perturbation can then be calculated using the results of Sec. IV.

To calculate the evolution of the flute amplitude $\xi(z,\tau)$, we write the beam breakup equation [12]

$$\left[\frac{\partial}{\partial z}\,\gamma\,\frac{\partial}{\partial z}+\gamma k_{\beta y}\right]\xi(z,\zeta)=\int_0^{\zeta} d\zeta'\,W_y'(\zeta'-\zeta)\,\xi(z,\zeta'), \tag{6.1}$$

where $W_y' \equiv \partial_y W_y$ is the wake function produced by a harmonic beam perturbation with wave number k_x and is proportional to the $\partial F_{y,n}/\partial_y$ given by Eq. (4.5), and $k_{\beta y}$ is the betatron wave number associated with the applied vertical focusing. Since we are considering beams with small phase extent (in the fundamental accelerating wave), $W_y \propto \sin(k_n\zeta) \propto k_n\zeta$. Following Whittum, the asymptotic flute amplitude for a coasting beam ($\gamma=$ constant) due to the nth antisymmetric mode is found by a saddle-point analysis of Eq. (6.1) to be, in the limit of strong focusing (instability growth length L_g satisfying $k_{\beta y}L_g>1$),

$$\xi(z,t)\propto \exp\frac{3\sqrt{3}}{4}\left(\frac{Y_{\perp,n} z\,\tau^2}{\gamma k_{\beta y}}\right)^{1/3}, \tag{6.2}$$

where

$$Y_{\perp,n}=\frac{r_e}{4\pi^2}\,\frac{N}{\sigma_z\sigma_x}\,c^2 k_n\,\frac{\partial F_{y,n}}{\partial y}; \tag{6.3}$$

r_e is the classical electron radius, and N is the number of electrons per bunch. As an example, relevant to experimentation in a 10.6-μm wavelength accelerator similar in design to that considered in Ref. [2], we choose a structure and beam with $a=5\ \mu$m, $b=6.05\ \mu$m, $\sigma_x=100\ \mu$m, $k_{\beta y}=5\ \mathrm{cm}^{-1}$ (equilibrium beta function $\beta_{y,\mathrm{eq}}=k_{\beta y}^{-1}=2$ mm), $N=10^5$, and $\gamma=100$. Using the mode with highest coupling to the dipolelike mode (near $k_x \approx a^{-1}$) we find a growth length of $L_g=8$ cm, which justifies the strong focusing approximation.

It should be possible to stabilize this instability by use of horizontal focusing of sufficient strength to mix the horizontal positions of the beam particles in a time shorter that the growth time. This is quantified by condition $k_{\beta x}L_g>1$, which implies that the horizontal betatron wave number must scaled to the vertical by the ratio $k_{\beta y}L_g$, which in our example yields $k_{\beta x} \geq k_{\beta y}/40$.

This ratio may appear to be arbitrarily chosen, but it in fact may be constrained by other considerations—primarily that the beam be in thermal equilibrium. Because the tranverse wakes in this case couple the x and y motion in a nonlinear fashion, one may expect that if the temperature is different in the two dimensions that it would soon equalize. In terms of standard beam characteristics, this proposed requirement $T_x=T_y$ is equivalent to $\epsilon_x/\beta_{\mathrm{eq},x}=\epsilon_y/\beta_{\mathrm{eq},y}$, or $\epsilon_x=\epsilon_y(k_{\beta y}/k_{\beta x})\approx\epsilon_y(k_{\beta y}L_g)$. This in turn implies a constraint on the beam sizes, as $\sigma_x/\sigma_x=\sqrt{k_{\beta x}\epsilon_y/k_{\beta y}\epsilon_x} \approx k_{\beta y}L_g$, which is approximately 40 in our case. This is a borderline problem for our example, in that $\sigma_y \approx \sigma_x/40 = 2.5\ \mu$m, which only one-fourth of the total vertical gap in the structure. This potential problem, which demands rigorous analysis in future work, certainly emphasizes the need to have very strong vertical focusing in the device.

The problem of instabilities due to long range wake fields can be studied using the multibunch BBU formalism previously developed by Thompson and Ruth [13]. We employ a strongly damped wake approximation, the daisy-chain

model, where a bunch is only affected by the wake fields from the previous bunch. For optical accelerators, the horizontal diffraction of the wakes make this model promising; on the other hand, since each bucket will undoubtedly be filled in such a short wavelength device, the wakes must be very heavily damped or have large frequency spreads in the relevant modes for the model to be accurate. We additionally assume that the high-frequency wakes responsible for the single-bunch flute instability are ignorable from the multibunch point of view, again because the enhanced diffraction of these components of the wake fields quickly dampen their effect on the bunch train.

In order to include the effects of acceleration and adiabatic damping, it is convenient to define an effective distance $z_{\rm eff}=k_{\beta y}^{-1}(0)\int_0^z k_{\beta y}(z')dz'$, where the betatron wave number now is considered as a function a distance z down the structure. Assuming $k(z)=\sqrt{\gamma(0)/\gamma(z)}k(0)$, with the approximation that the energy is much greater at the end of the structure than at the beginning, the effective distance becomes $z_{\rm eff}=2\sqrt{\gamma_0 z/\gamma'}$, where $\gamma'=eE_{\rm acc}/m_e c^2$ is the normalized accelerating gradient. The equations of motion in the effective length approximation become [13]

$$\frac{\partial^2 y_1}{\partial z_{\rm eff}^2}+k_{\beta y}^2 y_1=0,$$

$$\frac{\partial^2 y_n}{\partial z_{\rm eff}^2}+k_{\beta y}^2 y_n=\frac{N r_e}{\gamma}\,\frac{1}{2\pi\sigma_x}\,\frac{\partial F_y}{\partial y}\,y_{n-1}, \tag{6.4}$$

where the first bunch is explicitly unaffected by transverse wake fields. Assuming solutions of the form $\gamma_n=A_n e^{ikz}$, it is found the deflecting amplitude A_n grows with effective growth length is approximately $L_{g\rm eff}=4\pi\sigma_x(\gamma/Nr_e)k(\partial F_y/\partial y)^{-1}$. We again use the parameters $\sigma_x=100\ \mu$m, $N=10^5$, and $\gamma(0)=100$, which assuming every optical accelerating ''bucket'' is filled, and that the accelerating gradient is $eE_{\rm acc}=1$ GeV/m, implies we have a beam loaded $Q=10^3$, similar to the expected unloaded Q of the optical structure itself [2]. For $k_{\beta y}=5\ {\rm cm}^{-1}$, the growth length of the multibunch BBU instability is 15 cm. This is relatively gentle growth, which can be controlled by a variety of methods [13], including detuning of the dipole mode frequencies, and tuning the strongest frequencies near half-integer harmonics of the accelerating frequency, thus placing the bunches near zero crossings of the dipole-mode wakes.

VII. DISCUSSION

The results we have obtained above allow much greater freedom in imagining linear accelerator designs at much shorter wavelengths, as they mitigate the scaling [14] of the transverse wake coupling strength which limits the current in these devices, from $W_\perp'\propto k_\perp^3\propto k_0^3$ ($k_\perp$ is the transverse wave number of the mode, analogous to our present k_x) in the cylindrical case, to $W_\perp'\propto k_x^3\propto\sigma_x^{-3}$ (at a constant beam charge), independent of accelerating wavelength in the slab geometry for the case of multibunch BBU. The scaling of the flute instability is is a bit less dramatic, $W_\perp'\propto k_x^3\propto\sigma_x^{-2}k_0$, and indeed we see that the growth of the flute instability is a bit stronger than for multibunch BBU.

TABLE I. Comparison multibunch BBU of a cylindrical and slab-symmetric linear accelerator with an average accelerating gradient of 1 GeV/m, fundamental wavelength $\lambda_0=2\pi/k_0=10.6\ \mu$m, $a=2.5\ \mu$m, and beam loading quality factor $Q=1000$; only the lowest frequency dipolelike mode is considered, with $\sigma_x=100\ \mu$m in the slab case. Comparison parameters: average current eNc/λ_0, transverse wake strength $W_\perp'/eN$, and BBU growth length L_g.

	Slab case	Cylindrical case
Average current	490 mA	16 mA
Transverse wake (dominant dipole)	30 V/(mm^2 fC)	10^5 V/(mm^2 fC)
Multibunch BBU growth length	15 cm	1.4 cm

Alternatively, if we allow the beam charge to be varied, one can see that, by spreading the beam out in one dimension while keeping efficient coupling of the accelerating wave to the structure in the narrow dimension, much more charge per bunch can be accelerated. This comes at a price, of course, which is that the electromagnetic stored energy is much larger in the case of a slab-symmetric device as opposed to a cylindrically symmetric accelerator of equivalent beam hole dimension—the shunt impedance of the slab-symmetric accelerator is very low. At optical or infrared wavelengths, however, the stored energy is not a problem, as laser powers large enough to drive ultrahigh accelerating fields in slab-symmetric structure are easily obtainable, and the useful field amplitudes are limited by structure breakdown considerations [15]. In the slab-symmetric case the low shunt impedance can be understood as being due to a large number of equivalent cylindrically symmetric accelerators operating in parallel, yielding a small impedance.

This multiple-channel, parallel accelerator is a useful analogy for helping understand the transverse wake fields as well. It is true that the transverse impedance that the beam ''sees'' at the highest transverse coupling to the structure ($k_x\approx a^{-1}$) is very close to that of the cylindrical structure of the same vacuum radius a, and so the beam breakup is similar—the flute instability is nearly identical for the portion of the beam within $\Delta x\sim 2a$ as for single-bunch BBU for the same charge beam in the equivalent cylindrically symmetric structure. The advantage of the slab-symmetric structure is twofold, however; it allows much more beam charge to be accelerated for the equivalent BBU problem, and the flute BBU can be stabilized by a mechanism, horizontal mixing, that is unavailable in the cylindrically symmetric structure. In addition, if the flute instability is stabilized, then the multibunch BBU is much more stable, for equivalent beam loading, than the cylindrically symmetric accelerator.

To illustrate this point, we give a list of parameters describing two equivalent designs with slab and cylindrical geometry, respectively, in Table I. In both designs, we obtain a linear accelerator with an average accelerating gradient of 1 GeV/m, wavelength $\lambda_0=2\pi/k_0=10.6\ \mu$m, the beam half-gap $a=5\ \mu$m, and beam loading quality factor $Q=1000$. It can be seen that in the slab case, with a beam width of $\sigma_x=100\ \mu$m, much higher average current can be accelerated

at this beam loading level, and it can be propagated stably longer.

VIII. CONCLUSIONS

In conclusion, we have theoretically and computationally analyzed the transverse wake fields in a slab-symmetric dielectric-loaded structure. We have found and quantified the suppression of the transverse wake fields for wide beams in these structures, using infinite beam, harmonic beam, and Gaussian beam models, and made an analysis of the beam breakup instability in this type of structure. The additional advantages of using wide beams in a slab symmetric structure for accelerating larger beam currents was noted as a byproduct of this analysis. While we have concentrated on laser-driven optical or infrared accelerators, as they are likely to use dielectrics, the conclusions reached are quite general, and should be easily applied to submillimeter wave metallic cavity structures as well.

The results we have presented allow more serious consideration of short-wavelength advanced accelerator schemes, which have potential application to linear colliders as well as radiation-producing accelerators (free-electron lasers, Compton scattering x-ray sources, etc.). These advantages, we believe, present significant motivation for further theoretical and experimental work in this field; we are presently working on a test of these results using asymmetric, high charge beams, which produce cm wavelength wake fields, as well as an improved analysis of instabilities in slab-symmetric accelerators.

ACKNOWLEDGMENTS

The authors have benefitted from discussions with A. Chao, W. Gai, H. Henke, and L. Serafini. This work was supported by the U.S. Department of Energy under Grant Nos. DE-FG03-93ER40796 and W-31-109-ENG-38, and the Alfred P. Sloan Foundation under Grant No. BR-3225.

[1] D. Yu *et al.*, in *Advanced Acceleration Concepts*, edited by P. Schoessow (AIP, New York, 1995), Vol. 335, p. 800.
[2] J. Rosenzweig *et al.*, Phys. Rev. Lett. **74**, 2467 (1995).
[3] W. K. H. Panofsky and W. A. Wenzel, Rev. Sci. Instrum. **27**, 967 (1956).
[4] J. B. Rosenzweig *et al.*, Phys. Rev. A **39**, R1586 (1989).
[5] M. Hogan and J. B. Rosenzweig, in *Proceedings of the 1993 IEEE Particle Acceleration Conference*, edited by S. T. Corneliussen (IEEE, New York, 1993), Vol. 5, p. 3494.
[6] W. Gai *et al.*, Phys. Rev. Lett. **61**, 2756 (1988).
[7] K. Y. Ng, Phys. Rev. D **42**, 1819 (1990).
[8] E. Chojnacki *et al.*, in *Proceedings of the 1993 IEEE Particle Acceleration Conference* (Ref. [5]), Vol. 2, p. 815.
[9] Two articles discussing the vanishing of transverse wakes in the pure slab symmetric limit are by A. Tremaine *et al.* and A. W. Chao *et al.*, in *Proceedings of the 1996 DPB/DPF Summer Study on New Directions for High-Energy Physics* (Stanford University Publications, Palo Alto, CA, 1997), p. 399 and p. 374, respectively.
[10] R. Ruth *et al.*, Part. Accel. **17**, 171 (1985); K. Bane *et al.*, IEEE Trans. Nucl. Sci. **32**, 3524 (1985).
[11] R. Siegman, in *Lasers* (University Science, Mill Valley, CA, 1986).
[12] D. Whittum, Phys. Rev. A **46**, 6684 (1992).
[13] K. A. Thompson and R. D. Ruth, Phys. Rev. D **41**, 964 (1990).
[14] R. Palmer, Annu. Rev. Nucl. Part. Sci. **40**, 529 (1990).
[15] D. Du *et al.*, Appl. Phys. Lett. **64**, 3073 (1994).